Poster ID: Mon-Mo-Po1.10-03[111]

YOKOHAMA National University

[ver.1.0]

Rotation Test of an Integrated Magnetic Bearing Using Multiple HTS Cubic Bulks Units.

K. Yamagishi[1], J. Ogawa[2]

1: Yokohama National University, Kanagawa, 240-8501, Japan.

2: Niigata University, Niigata, 950-2181, Japan.

Abstract

For magnetic bearings combining multiple cubic superconducting bulks, placement is a crucial factor. In this paper, the magnetic bearing surface constructed by arrangement optimization was composed of eight superconducting cubic bulk units. The combined arrangement of cubic superconducting bulks was determined by optimizing the spatial uniformity of the magnetic bearing' s trapped magnetic flux distribution. We constructed a physical model in which a permanent magnet in the form of a floating rotor was sandwiched from above and below by an integrated magnetic bearing surface. Using rotation test equipment and an encoder, we investigated the influence of an optimal arrangement index on rotation loss that occurs due to magnetic flux distribution nonuniformity. In addition, the rotation axis tilt angle due to nonuniform magnetic flux distribution was measured using a laser displacement meter.

1.Overview of Integrated Superconducting Bulk Magnetic Bearings.

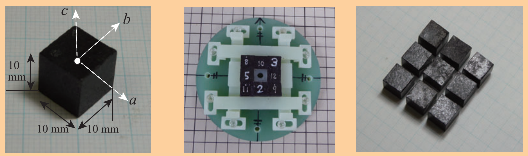

(a) Basic cubic bulk. (b) Three-row, three-column square arrangement of cubic bulks.

The magnetic bearing used in this experiment is a floating rotor using a composite superconducting bulk bearing surface consisting of multiple cubic bulk units and a cylindrical permanent magnet. The magnetic bearing surface is composed of cubic bulk units as shown in the figure (a) above, and is arranged as shown in (b). This bearing surface has a square arrangement consisting of nine blocks as shown in figure (b), and one of the centers is a spacer made of Glass Fiber Reinforced Polymer (GFRP) with a hole through which the rotor's rotating shaft passes.

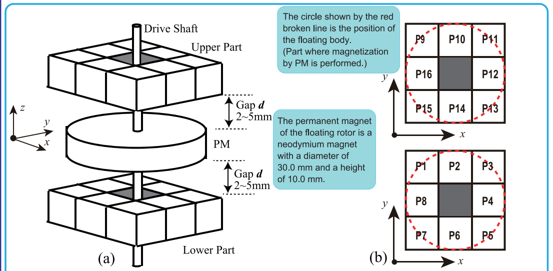

This cubic bulk placement method is determined by the "method of calculating the optimal placement" that we have studied previously*.
The model is based on a previous model in which two bearing surfaces constructed in this way were used to sandwich a permanent magnet in the form of a floating rotor from above and below.
The figure on the left shows the entire bearing that combines these parts. As shown in figure, the upper and lower parts are each selected from the 16 cubic bulks shown in Table I, and the inclination of the levitating body with respect to the rotation axis is controlled by the calculated combination pattern.

Table I . Specification of HTS Cubic Bulks.

Cube bulk	B_{tc} (T)	Cube bulk	B_{tc} (T)	Cube bulk	B_{tc} (T)	Cube bulk	B_{tc} (T)
Cb11	0.125	Cb12	0.130	Cb13	0.129	Cb14	0.114
Cb21	0.106	Cb22	0.106	Cb23	0.095	Cb24	0.103
Cb31	0.124	Cb32	0.122	Cb33	0.120	Cb34	0.121
Cb41	0.093	Cb42	0.100	Cb43	0.091	Cb44	0.096

2. Optimal Placement of Bulks.

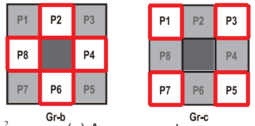

(a) Arrangements.

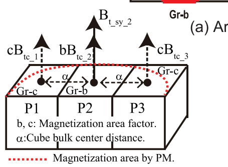

(b) Magnetic field calculation considering the influence of adjacent bulks.

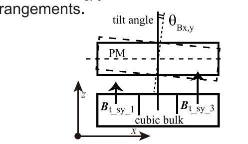

(c) Calculation of the inclination of the rotating shaft of the floating rotor by the combined magnetic field.

Regarding the arrangement of the cubic bulk on the magnetic bearing surface, it is necessary to calculate the magnetic field for the optimal arrangement so that the magnetic flux distribution is uniform, considering that adjacent bulks affect one another' s magnetic flux. In this calculation, the magnetic field is calculated for each position of the arranged bulk, with the influence of magnetization by the permanent magnet and by the adjacent bulk taken into account (Figure (a), (b)). In these calculations, the optimal placement pattern was calculated when the values of θBx and θBy of the constraint condition were changed to approximately 1–5 degree. Table II shows the optimal arrangement pattern based on the calculation results.

TABLE II
CUBIC BULK ARRANGEMENT OBTAINED BY OPTIMAL CALCULATION.

Group	Position	$\|\theta_{Bx,y}\|$ [degree] < ~1 "Best"	~2	~3	~4	~5 "Bad"
Gr-c (Lower part)	P1	Cb23	Cb32	Cb12	Cb33	Cb31
	P3	Cb13	Cb23	Cb13	Cb32	Cb13
	P5	Cb24	Cb13	Cb24	Cb23	Cb44
	P7	Cb41	Cb41	Cb32	Cb31	Cb43
Gr-b (Lower part)	P2	Cb22	Cb21	Cb11	Cb44	Cb11
	P4	Cb11	Cb11	Cb22	Cb43	Cb12
	P6	Cb12	Cb12	Cb21	Cb42	Cb23
	P8	Cb21	Cb22	Cb23	Cb21	Cb41

Group	Position	$\|\theta_{Bx,y}\|$ [degree] < ~2 "Best"	~2	~2	~2	~3 "Bad"
Gr-c (Upper part)	P9	Cb31	Cb34	Cb14	Cb22	Cb34
	P11	Cb34	Cb24	Cb41	Cb24	Cb42
	P13	Cb33	Cb31	Cb31	Cb14	Cb22
	P15	Cb32	Cb33	Cb43	Cb41	Cb14
Gr-b (Upper part)	P10	Cb42	Cb14	Cb33	Cb13	Cb32
	P12	Cb14	Cb44	Cb42	Cb34	Cb21
	P14	Cb43	Cb42	Cb34	Cb12	Cb33
	P16	Cb44	Cb43	Cb44	Cb11	Cb24

3. Rotation Test.

A. Overview of Test Equipment.

For the magnetic bearing parts used in the rotation test, two upper and lower bearing surfaces constructed using the optimal arrangement method described in the previous section were incorporated into the rotation test equipment.

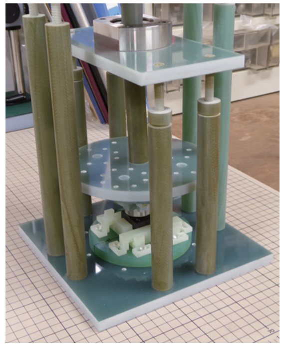

(a) Photo of test equipment.

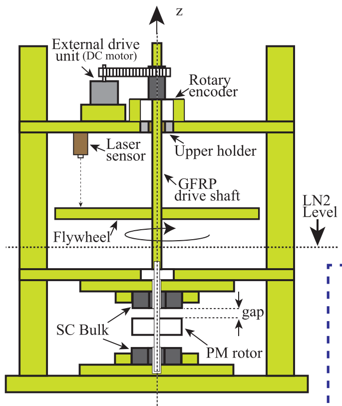

(b) Illustration of test equipment.

Rotation test equipment incorporating HTS bulk integrated magnetic bearings.

The rotating shaft is supported by the upper rotating shaft holder and is connected to the rotating shaft of the floating rotor near its center.
A GFRP flywheel was connected to the rotor. The flywheel was discshaped with a diameter of 150 mm and a height of 10 mm, and weighed 342 g.
The control signal of the DC motor for driving the test equipment was processed by a PC via a dedicated control board, as were the measurement data from the rotary encoder and laser sensor.
The laser sensor measured the tilt of the rotating shaft, targeting the flywheel integrated with the rotating shaft.

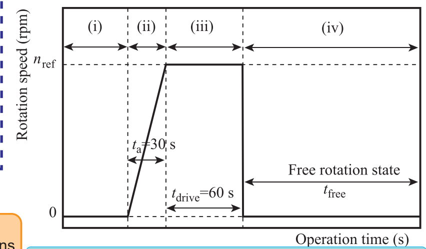

Operation sequence of rotation test. The operation sequence is divided into the following four parts. (i) Stop, (ii) Acceleration, (iii) Constant speed rotation, (iv) Free rotation. nref: Rotational speed command value.

B. Measurement Result of Rotation Test.

First, the test equipment was driven, and the rotational speed range over which stable operation was possible was measured. A comparison was made between two combinations of "Best" and "Bad" .
In the case of the "Best" combination, the maximum speed at which stable operation was pos-sible was 450 rpm. At higher speeds, vibration increased, and the system became unstable. The maximum stable speed for the "Bad" combination 398 rpm.

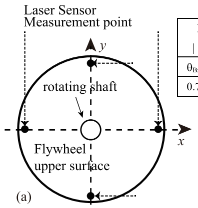

Best: $\|\theta_{Bxy}\|$<1		Bad: $\|\theta_{Bxy}\|$<5	
θ_{Bx}	θ_{By}	θ_{Bx}	θ_{By}
0.7	0.5	1.2	0.9

(b)

The tilt angle of the rotation axis was measured using a laser sensor. The laser sensor attached to the case of the rotation test device measured the distance to the rotating surface on the upper surface of the flywheel directly connected to the rotating shaft. Figure (a) shows the measured points. The measurement results are shown in figure (b).
The tilt angle of the rotation axis of the combination of "Best" and "Bad" was close to the optimum value, but the difference was small.

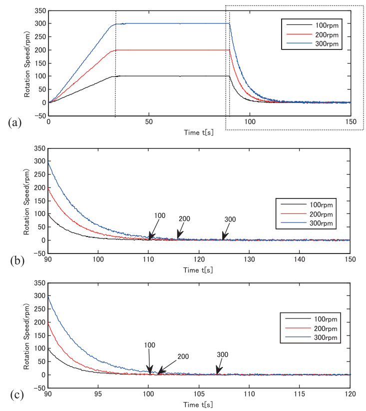

Measurement result of rotation speed using the rotation test equipment. a) The rotation speed of the whole test. (b) Rotational speed during free rotation. "Best" combination. (c) "Bad" combination.

TABLE III
FREE ROTATION TIME DUE TO BULK ARRANGEMENT.

$\|\theta_{Bx,By}\|$ < (degree)	Gap d (mm)	Rotation speed(rpm)	Free rotation time(s)
1 [Best]	2	100	20
		200	25.7
		300	34.6
	5	100	10.3
		200	10.9
		300	16.6
5 [Bad]	2	100	16.8
		200	19.4
		300	24.5
	5	100	10.2
		200	10.8
		300	11.4

Table III shows the results of measuring the time until rotation stops in the free rotation state. The point indicated by the arrow in the graph is the point where the system stops. The time required to stop in the case of Fig. (B) and Fig. (C) becomes longer as the initial rotation speed is higher, but the result of Fig. (C) shows a shorter stop time overall. The Table III shows other similar results.
In addition, the gap between the bearing surface and the rotor has a longer stop time as the value of d is smaller.
In summary, the beneficial effects of optimal placement were confirmed, albeit slightly. It was also possible to confirm the relationship between the rotation stop time and the gap between the bearing surface and the rotor.

4.Discussion & Conclusions

We aimed to construct magnetic bearings using basic unit cubic bulks, with the goal of performing an optimization calculation of the configuration of bulks. The integrated bulk bearing constructed by this optimization calculation was constructed in two contrasting patterns, "Best" and "Bad," and a comparative examination was conducted using a rotation test. Simultaneously, the gap distance d between the bearing and the rotor was measured and compared. In the rotation test, the positive effect of optimal arrangement on the duration of the free rotation state was confirmed. However, observed differences between the two contrasting bulk arrangements were not as large as expected. There are several possible reasons for this.

(1) First, the difference between "Best" and "Bad" configurations was not particularly large, possibly due to an unexpected lack of variation in the magnetic properties of individual cubic bulks.

(2) Also, because the number of cubic bulks was small, the upper and lower parts of the bearing could not be optimized simultaneously.

(3) Observed differences between the two contrasting bulk arrangements may also have been minimal simply because natural variation (i.e., noise) in the performance of the other parts were more dominant in the rotation test than that of the bearing parts under investigation.

Acknowledgment :

This work was supported by JSPS KAKENHI Grant Number 24560325.